Evaluation of Mapping Accuracy of High-Resolution Stereoscopic Satellite Images

Hossam H. El-Semary[*]

Faculty of Engineering-Shobra , Benha University-Cairo-Egypt

Email: hossam.elsemary@feng.bu.edu.eg

Abstract

High resolution satellite images is still used in large scale mapping due to the need to produce fast products. High resolution stereoscopic satellite images present good enough 3d products that include the benefits of large-scale coverage and low-cost products. A stereopair of IKONOS satellite is used in this research that covers a part of North Sudan country. The study handles the 3d mapping accuracy of using stereoscopic satellite images. The study gives a spotlight on the accuracy in X, Y, Z and the space vector R. Another view of this study the N, E and elevation is indicated. The research environment is mainly ENVI software due to its capabilities of topographic processing module. Some distributed set of ground points (control and tie) was determined on the images and then observed using GPS surveying. Several experiments have been performed to evaluate the resulted mapping product.

Keywords: Stereoscopic; High Resolution; Satellite Images; Spatial Accuracy.

1. Introduction

Many satellites provide imagery with high impacts in various geomatics fields. Using stereoscopic satellite images with a good base over height ratio can produce a good Digital Elevation Model (DEM). On can mention IKONOS that has been successfully used for 3d mapping and objects extraction. If orthoimages are also generated or available, textured 3D models can be created and used for photo-realistic visualization [1]. Photogrammetric technique is an appropriate solution for obtaining the DEM of large areas. DEM data can easily be obtained using stereo images through photogrammetric methods [2]. The main objectives of this study are: To evaluate the mapping accuracy using high resolution stereoscopic satellite image. In addition; to generate the final DEM resulting from this system.

----

* Corresponding author.

2. Research Data

Stereoscopic products consist of two overlapped satellite images of a location on Earth, taken from two different perspectives position on the same track. IKONOS stereo pair contains an image collected at elevation angle above 60 degrees as well as an image collected at a higher elevation angle above 72 degrees with 30°-45° convergence with 0.54 to 0.83 base-to-height ratio. Figure 1 shows IKONOS image data collecting system with in track sampling.
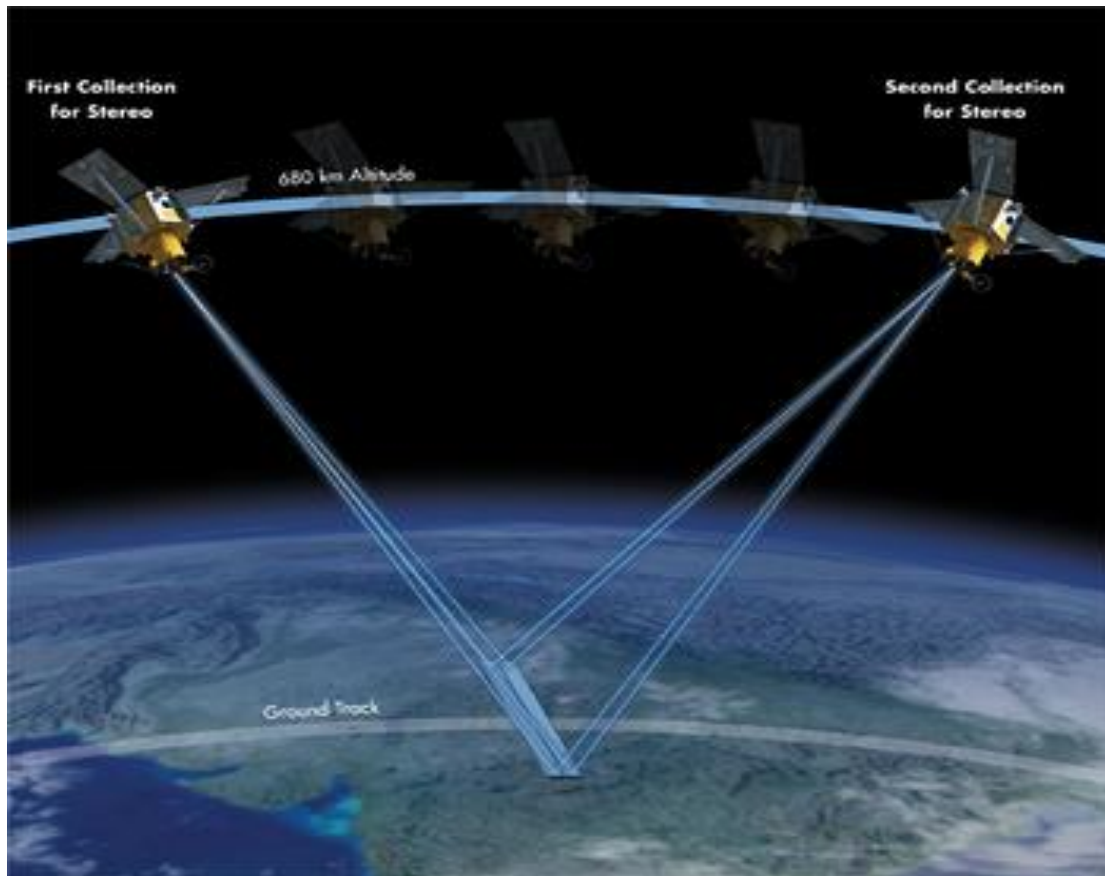

Figure 1: Stereo IKONOS Satellite Image data collection.

Reference Stereo products have a horizontal accuracy of 25 meters CE90 (Circular Error 90%) and a vertical accuracy of 22 meters LE90 (Linear Error of 90%) without any Ground Control Points (GCPs). When reliable GPS derived GCP is available the horizontal and vertical Geospatial accuracies increase to <2.5m horizontal and <1.5m vertical [3]. The test area (Wadi Seidna) is located at the north of Khartoum in Sudan bout 16km north of Omdurman city and geographically, it lies between upper left corner coordinates of (444535.977, 1747921.762) and lower right corner coordinates of (449800.083, 1742045.500). The elevation range of this area is about 60 m. The study area is about 31 Square Kilometers. Figures (2) and (3) show the general location of the study area. Table 1 indicates the relative polynomial coefficients for the stereo pair that can be used for image rectification model.
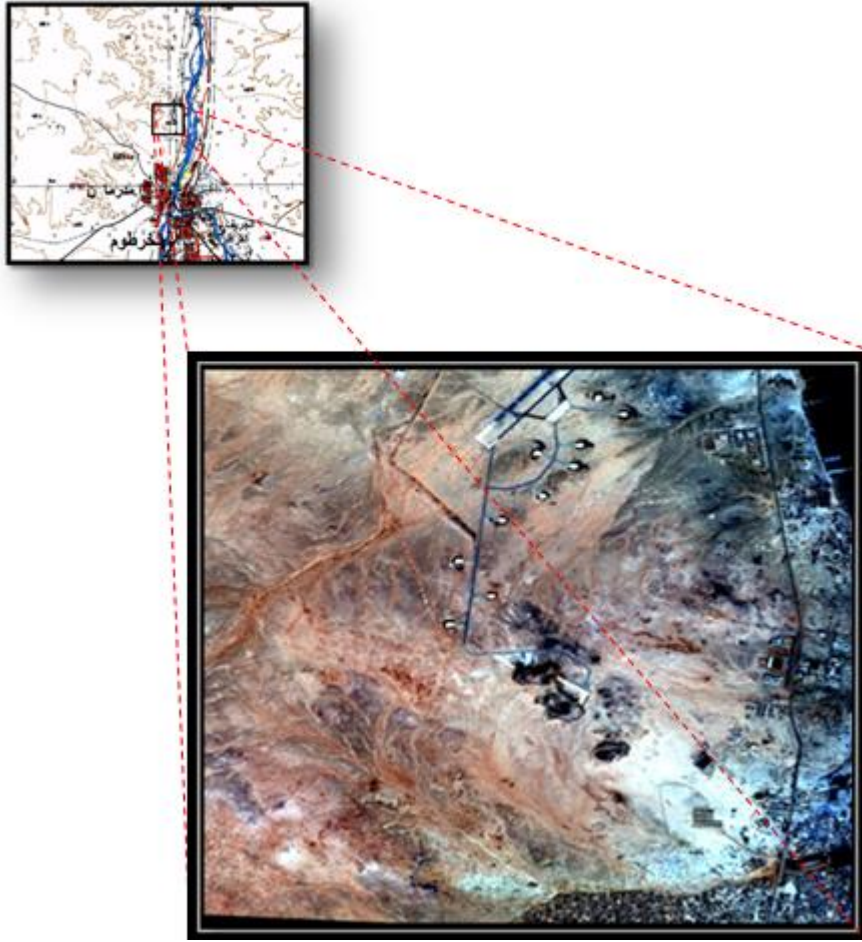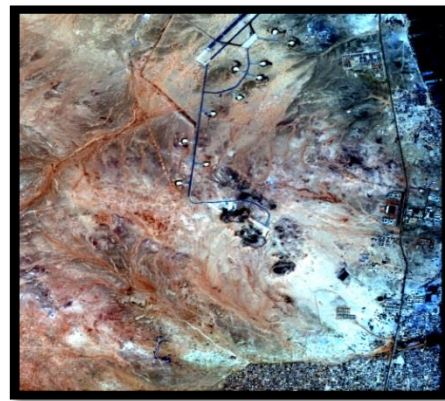
Figure 2: General location of the study area.

(a) Left Image   (b) Right Image

Figure 3: IKONOS HRS 1M stereo-pair of the study area.

Table 1: Main parameters of the available IKONOS HRS 1M stereo-pair.

Acquisition Date/Time	08:41 GMT 27-12-2003 and 08:42 GMT 27-12-2003
Sun Angle Azimuth	156.1241 and156.3809 degrees
Sun Angle Elevation	63.50707 and 47.50945 degrees
Overlap	99%
Rows	5893 and 6004 pixels
Columns	5351 and 5357 pixels
Pixel Size X	1.000 meters
Pixel Size Y	1.000 meters
Percent Component Cloud Cover	0
Size (km)	5.808 km * 5.344 km

3. Methodology

The developed system depends on input, output, processing and decision blocks and can be represented by flowcharting [4]. Figure 4 indicates the block diagram of the developed system where it is starting by input both left and right images to Envi (as a processing software). The GCPs must entered to carry out the rectification model and space resection by determining the stereopair parameters required for space intersection after. Then the space coordinates of the check (tie) points is calculated so accuracy assessment can be carried out by comparing its measured GPS coordinates with the calculated values. If the quality of the results is quite good the process can be stopped or a change in GCPs and tie points must be carried out.
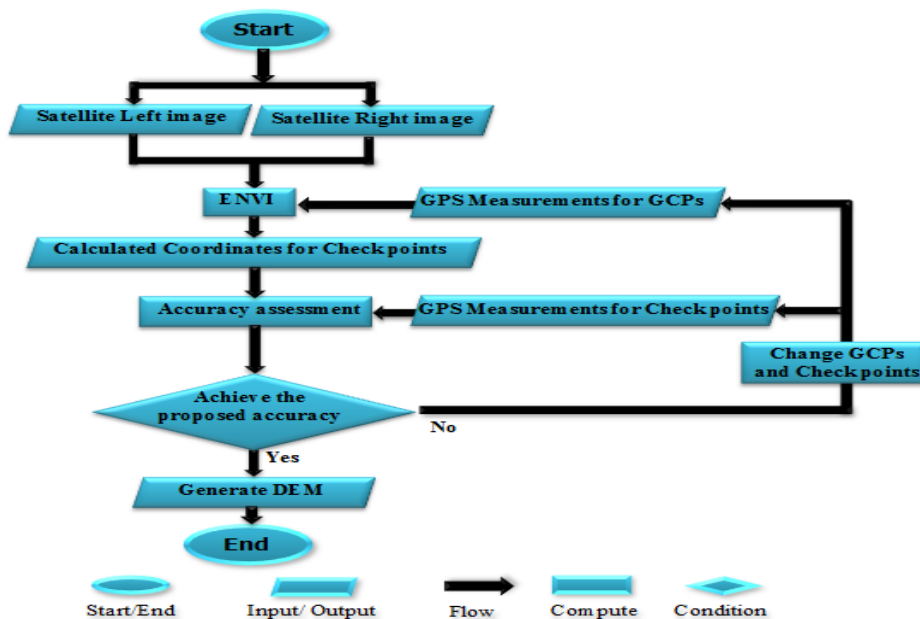

Figure 4: Block diagram of the research work.

The change may include elimination one or more GCPs according to how much it is far from the mathematical model (absolute error). If the result is accepted, then DEM of the study area can be generated using the same software of Envi. A lot of trials were made to reach the optimum case. Generation of DEM is a minor objective, so no accuracy assessment is established. Since the IKONOS satellite imagery vendor, Space Imaging Company, has not released the satellite ephemeris data, no physical mathematical model can be established. So, the most common applied mathematical model is the rational function model (RFM). The Rational Function Model (RFM) is a generalized model that is widely used. RFM has come into widespread use within the mapping community. The related research showed that both RFM and the polynomial model can reach reasonably satisfying accuracy. The RFM expresses each of the *x* and *y* image coordinates as a ratio of two polynomial functions. It can be represented as follows:

$$x = \frac{P1(X,Y,Z)}{P2(X,Y,Z)} = \frac{\sum_{i=0}^{m1}\sum_{j=0}^{m2}\sum_{k=0}^{m3} a_{ijk} X^i Y^i Z^i}{\sum_{i=0}^{n1}\sum_{j=0}^{n2}\sum_{k=0}^{n3} b_{ijk} X^i Y^i Z^i} \qquad (1)$$

$$y = \frac{P1(X,Y,Z)}{P2(X,Y,Z)} = \frac{\sum_{i=0}^{m1}\sum_{j=0}^{m2}\sum_{k=0}^{m3} c_{ijk} X^i Y^i Z^i}{\sum_{i=0}^{n1}\sum_{j=0}^{n2}\sum_{k=0}^{n3} d_{ijk} X^i Y^i Z^i} \qquad (2)$$

Where,

x,y	Image coordinates
X,Y,Z	Ground coordinates
$a_{ijk}, b_{ijk}, c_{ijk}, d_{ijk}$	Polynomial coefficients (total 80)
$m_1, m_2, m_3, n_1, n_2, n_3$	0-3 , where $i+j+k \leq 3$

The polynomial coefficients are called rational function coefficients (RFCs). The RPCs are calculated by Space Imaging from the satellite ephemeris and attitude data instead of releasing the ephemeris data themselves. Therefore, the RFM model is implemented by most of the commercial software packages to use the supplied RPCs. This software modules deal with IKONOS satellite images by reading the RPC files and applying the RFM model to orient the IKONOS imageries. Static relative GPS positioning technique was used for measuring the ground control points. Two well identified points of the High Accuracy Reference Network provided by the Sudanese Survey Authority, near the study area, were chosen as reference stations. Ten out of twenty-two points were selected to be ground control points and the other twelve points were used as check points. Figure 4 shows the whole set of the measured ground points while Figure 5 shows the distribution of control and check points. Geo-referencing and stereo-model setup of the images was established using different numbers and different distribution of GCPs until get the best accuracy of 10 ground control points. The 10 pyramid points represent the Ground Control Points, while the rest of the points (rounded points are used as check points). Point 1 lies on the border of the stereopair so it is marked with red pyramid in figure 4.
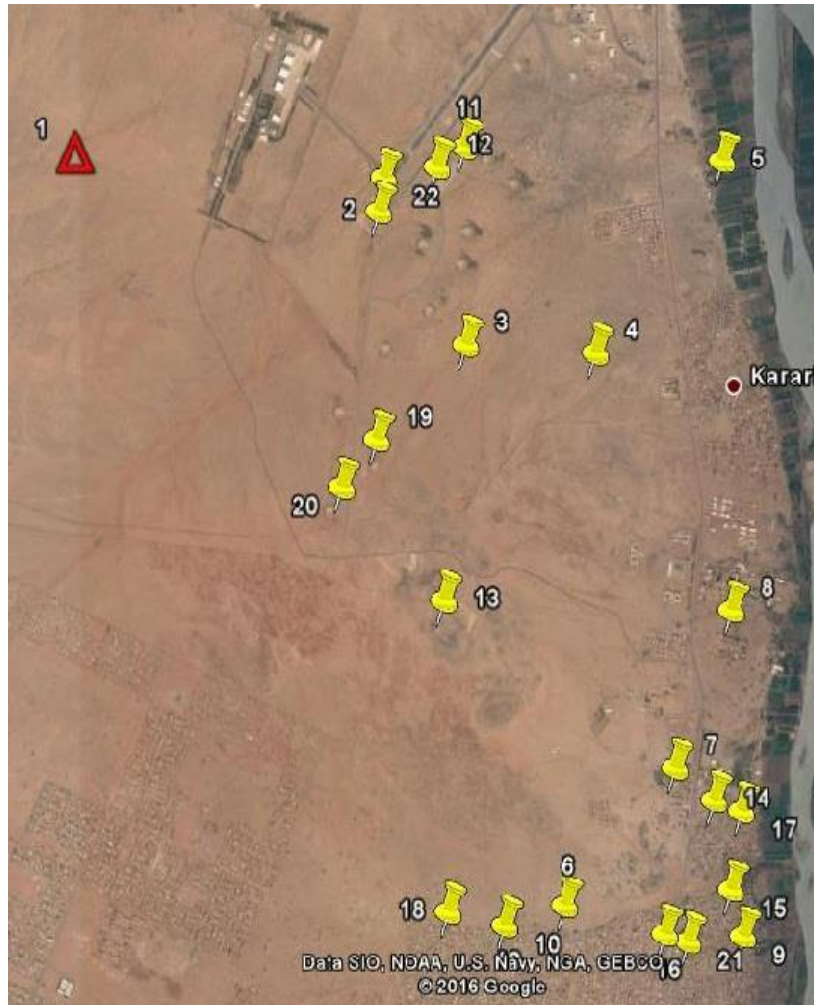
Figure 5: Ground control points and check points.

The final GPS coordinates of ground control and check points are listed in table 2 in the format of easting, northing and height (E, N, H). The red color is used for control and green color is used for check points.
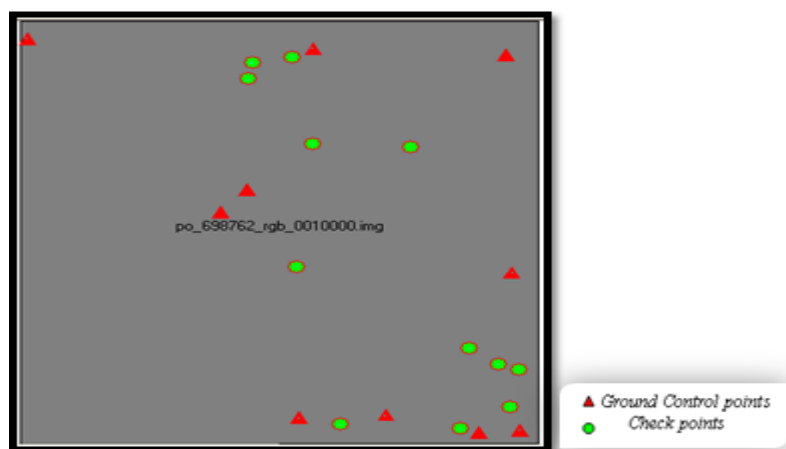

Figure 6: Selected Ground control points & check points.

Table 2: Final GPS coordinates for both GCPs and check points.

NO	ID	Type	Easting	Northing	Height
1	GCP28	Control	449548.020	1747432.638	381.723
2	GCP29	Control	444593.142	1747670.157	404.44
3	GCP27	Control	449694.505	1742120.183	384.672
4	GCP43	Control	447409.125	1742295.875	388.773
5	GCP44	Control	446865.860	1745528.241	402.499
6	GCP45	Control	449610.442	1744352.352	386.826
7	GCP46	Control	446593.192	1745203.946	405.533
8	GCP48	Control	448312.423	1742333.837	386.439
9	GCP49	Control	447552.933	1747529.038	391.878
10	GCP50	Control	449268.7255	1742087.394	385.938
11	CP30	Check	447336.227	1747394.633	393.181
12	CP33	Check	446924.385	1747321.87	394.619
13	CP34	Check	447381.562	1744428.317	436.551
14	CP36	Check	448561.519	1746118.83	390.771
15	CP35	Check	447557.070	1746175.505	395.371
16	CP37	Check	449603.553	1742438.988	383.786
17	CP38	Check	449472.709	1743051.137	383.910
18	CP39	Check	449685.294	1742977.897	382.444
19	CP41	Check	449088.085	1742137.513	385.269
20	CP47	Check	447846.782	1742200.025	390.105
21	CP32	Check	446886.200	1747091.386	395.575
22	CP42	Check	449171.625	1743275.145	385.820

To apply the mapping accuracy assessment; the following equations is used by computing the RMS error in easting, northing directions and height respectively.

$$RMSeE = \sqrt{\frac{1}{n}\sum_{i=1}^{n} \Delta Ei^2} \qquad (3)$$

$$RMSeN = \sqrt{\frac{1}{n}\sum_{i=1}^{n} \Delta Ni^2} \qquad (4)$$

$$RMSeZ = \sqrt{\frac{1}{n}\sum_{i=1}^{n} \Delta Zi^2} \qquad (5)$$

RMSeE =   Root Mean Square error in E direction

RMSeN =   Root Mean Square error in N direction

$RMSeZ =$ Root Mean Square error in Z

$\Delta Ei=$ the X Residual for GCP i

$\Delta Ni=$ the Y Residual for GCP i

$\Delta Zi=$ the Z Residual for GCP i

$i =$ GCP Number

$n =$ the number of GCP

4. Results and Analysis

Figure (5) shows the final rectified layered map produced using manual selection to guarantee the high performance. Ten points were chosen to testify the performance of the mapping accuracy. Table (3) indicates the results of the selected testing ground points.

The average absolute error is computed and found equal to 0.5814 m in E while it was 0.5369 m in N and equals 0.8372m in total planimetric.

This result is near 1.5 ground pixel size of the satellite image. Another way to indicate the results is the standard deviation which was 0.333287624 m in E while it was 0.226860508 m in N and 0.294663469 m in total planimetric. This result is near 0.5 ground pixel size of the satellite image.

Table 3: results of the selected ground points.

| NO	Name	E *map*(m)	N *map*(m)	E GPS(m)	N GPS(m)	RE(m)	RN(m)	TOTAL(m)
1	GCP 11	449684.000	1742978.340	449685.295	1742977.897	-1.295	0.443	1.368
2	GCP 12	447553.505	1747528.516	447552.933	1747529.038	0.572	-0.522	0.774
3	GCP 13	449695.200	1742119.531	449694.505	1742120.183	0.695	-0.652	0.952
4	GCP 14	446593.784	1745204.606	446593.192	1745203.946	0.592	0.660	0.886
5	GCP 15	449548.480	1747432.320	449548.020	1747432.638	0.460	-0.318	0.559
6	GCP 16	444592.960	1747669.730	444593.142	1747670.157	-0.182	-0.427	0.464
7	GCP 17	448312.860	1742333.630	448312.423	1742333.837	0.437	-0.207	0.483
8	GCP 18	446865.990	1745527.170	446865.86	1745528.241	0.129	-1.071	1.078
9	GCP 19	447847.237	1742199.598	447846.78	1742200.025	0.455	-0.427	0.623
10	GCP 20	449611.439	1744351.71	449610.44	1744352.352	0.997	-0.642	1.185
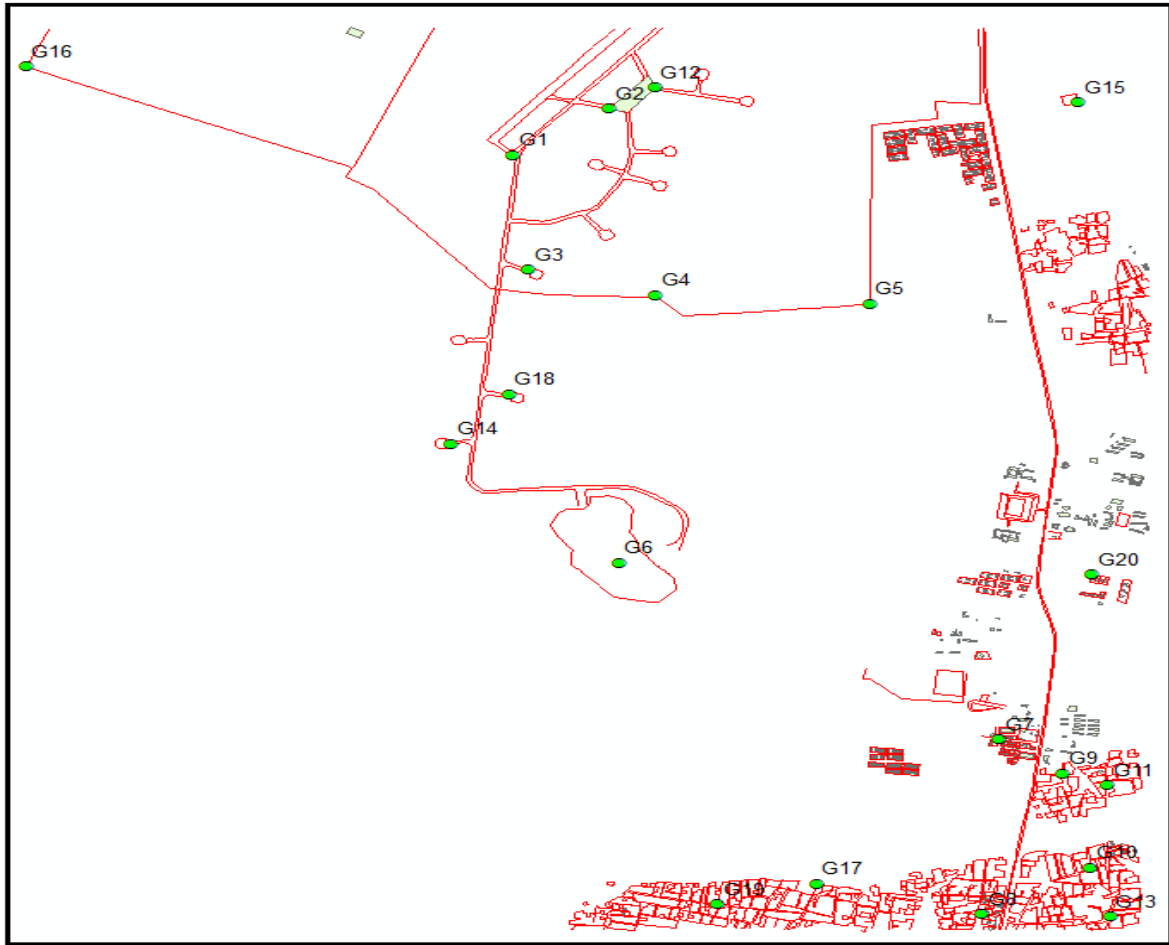
Figure 7: Final Rectified layered map for the study area.

5. Conclusion

One can conclude that the accuracy of the mapping product using stereo satellite images can reach to 1.5 of ground pixel size so the user of this type of products can take this information in his consideration. Using the standard deviation in this study gives another way to understand the accuracy limits of mapping process from stereo satellite images. One can conclude that 0.5 standard deviation of the ground pixel size is the accuracy limits for this type of products. In general one can conclude that it is good to make mapping using stereoscopic satellite images in geodetic and topographic mapping products but it is not convenient to use it in cadastral mapping products

6. Recommendations

It's necessary to recommend using stereoscopic satellite images in the production of small scaled mapping products (topographic or geodetic maps). It is not recommended to use stereoscopic satellite images in cadastral mapping due to the lack of accuracy comparing with unmanned aerial vehicles (UAVs). One

must recommend the comparison between stereoscopic satellite imagery and RADAR imagery.

References

[1]. A. Serwa, Automatic Extraction of Topographic Features from Digital Images. PhD thesis, Cairo: Faculty of Engineering in Cairo- Azhar University, 2009.

[2]. Tridipa Biswas, Kamal Pandey, Annadurai R., "Satellite Photogrammetry based DEM Generation using Satellite Stereo Pair Images and Terrain Parameters Extraction," Int. Journal of Advances in Remote Sensing and GIS,, vol. 4, no. 2, pp. 64-76, 2016.

[3]. S. I. Corporation, "IKONOS Stereo Satellite Imagery," 19 July 2012. [Online]. Available: www.satimagingcorp.com.svc/ikonos-stereo-satellite-image.html.

[4]. A. Serwa and H. Semarry, "Integration of Soft Computational Simulator and Strapdown Inertial Navigation System for Aerial Surveying Project Planning," Spatial Information Research (SPIR), vol. 24, no. 3, p. 279–290, June 2016.

[5]. A. Serwa, "Development of Soft Computational Simulator for Aerial Imagery Project Planning," Surveying and Land Information Science (SaLIS), vol. 75, no. 2, 2016.

[6]. K. Murthy, M. Shearn, B. D. Smiley, A. H. Chau, J. Levine and D. and Robinson, "Skysat-1: very high-resolution imagery from a small satellite.," International Society for Optics and Photonics, 2014.

[7]. Michael Xie, Neal Jean, Marshall Burke, David Lobell, and Stefano Ermon, "Transfer Learning from Deep Features for Remote Sensing and Poverty Mapping," in AAAI Conference on Artificial Intelligence (AAAI-16), 2016.

[8]. M. Jordan, "Why the logistic function? A tutorial discussion on probabilities and neural networks," Massachusetts Institute of Technology, Massachusetts, 1995.

[9]. B. DasGupta and G. Schnitger, the Power of Approximating: A Comparison of Activation, Advances in Neura Information Processing Systems ed., San Mateo, CA: Morgan Kaufmann Publishers, 1993.

[10]. C. Özkan and F. S. Erbek, "The Comparison of Activation Functions for," Photogrammetric Engineering & Remote Sensing, vol. 69, no. 11, p. 1225–1234, 2003.

[11]. Wang, Qian; Wang, Yi; Niu, Ruiqing; Peng, Ling, "Integration of Information Theory, K-Means Cluster Analysis and the Logistic Regression Model for Landslide Susceptibility Mapping in the Three Gorges Area, China," Remote Sensing, vol. 9, no. 938, p. 9, 2017.

[12]. Charlotte Pelletier, Silvia Valero, Jordi Inglada, Nicolas Champion, Claire Marais Sicre and Gérard Dedieu, "Effect of Training Class Label Noise on Classification Performances for Land Cover Mapping with Satellite Image Time Series," Remote Sensing, vol. 9, no. 2, p. 2, 2017.

[13]. Ratna Sari Dewi, Wietske Bijker, Alfred Stein and Muh Aris Marfai, "Transferability and Upscaling of Fuzzy Classification for Shoreline Change over 30 Years," Remote Sensing, vol. 10, no. 9, p. 1377, 2018.